Universal consequences of the presence of excluded volume interactions in dilute polymer solutions undergoing shear flow

2 AUTHORS, INCLUDING:

Satheesh Krishnan Nair Kumar
University of Kerala
18 PUBLICATIONS   114 CITATIONS

Universal consequences of the presence of excluded volume interactions in dilute polymer solutions undergoing shear flow

K. Satheesh Kumar* and J. Ravi Prakash

Department of Chemical Engineering, Monash University, Clayton, Victoria–3168, Australia†

(Dated: February 2, 2008)

The role of solvent quality in determining the universal material properties of dilute polymer solutions undergoing steady simple shear flow is examined. A bead-spring chain representation of the polymer molecule is used, and the influence of solvent molecules on polymer conformations is modelled by a narrow Gaussian excluded volume potential that acts pair-wise between the beads of the chain. Brownian dynamics simulations data, acquired for chains of finite length, and extrapolated to the limit of infinite chain length, are shown to be model independent. This feature of the narrow Gaussian potential, which leads to results identical to a δ-function repulsive potential, enables the prediction of both universal crossover scaling functions and asymptotic behavior in the excluded volume limit. Universal viscometric functions, obtained by this procedure, are found to exhibit increased shear thinning with increasing solvent quality. In the excluded volume limit, they are found to obey power law scaling with the characteristic shear rate β, in close agreement with previously obtained renormalization group results. The presence of excluded volume interactions is also shown to lead to a weakening of the alignment of the polymer chain with the flow direction.

I. INTRODUCTION

The nature of the thermodynamic interactions between the monomers in a polymer chain and the solvent molecules in their neighborhood, determines the ensemble of spatial configurations adopted by the chain, and as a result, has a significant influence on all conformation dependent properties of polymer solutions. Extensive investigations of static polymer solutions has established that both the temperature of the solution and the molecular weight of the dissolved polymer, control the strength of these interactions. Indeed their influence can be combined together in terms of a single variable, the so-called *solvent quality* parameter, $z = v_0(1 - T_\theta/T)\sqrt{M}$, where, v_0 is a polymer-solvent system dependent constant, T is the temperature of the solution, T_θ is the theta temperature, and M is the molecular weight. At large values of z, usually termed the *excluded volume limit*, various properties of polymer solutions have been shown to obey power law scalings with molecular weight. On the other hand, at intermediate values of z (the *crossover* region), the behavior of a host of different polymer-solvent systems has been found to be collapsible onto universal master plots with a suitable choice of the constant v_0.[1,2,3,4]

The entire range of observed behavior has been successfully modelled by static theories of polymer solutions by mimicking the influence of the solvent molecules on the conformations of a polymer coil, with the help of a potential that acts pair-wise between the various parts of a polymer chain. Typically, by representing the linear polymer molecule by a bead-spring chain consisting of N beads connected together by $(N - 1)$ Hookean springs, more or less repulsion by the solvent molecules is accommodated by varying the magnitude of the pair-wise *excluded volume* interaction parameter, denoted here by z^*, between the beads.[5,6,7,8] In particular, by noting that $z^* \sim (1 - T_\theta/T)$, and $N \sim M$, a quantitative prediction of both the excluded volume limit and the crossover regime

behavior of a number of equilibrium properties has been achieved by analytical theories, with the help of the mapping $z = z^*\sqrt{N}$.

The growing recognition that polymer-solvent interactions also play a key role in determining the behavior of polymer solutions far from equilibrium is responsible for the recent appearance of a number of studies aimed at obtaining a better understanding of this phenomenon.[9,10,11,12,13,14,15,16,17,18,19,20,21,22] Due to the analytically intractable nature of the non-equilibrium theory, a majority of these investigations have been largely numerical in nature. As in the case of static theories, polymer-solvent interactions have been modelled with the help of an excluded volume potential, such as the Lennard-Jones potential, acting pair-wise between the different parts of the polymer chain. While a number of qualitative conclusions on the influence of excluded volume interactions have been drawn by these studies, a methodical program aimed at cataloging the universal behavior of polymer solutions in a variety of flow fields in terms of the solvent quality parameter z—as has been done at equilibrium—has not yet been attempted. Nevertheless, some progress in this direction has been made in the framework of approximate analytical theories. In the excluded volume limit, Öttinger and co-workers[9,10,23] have examined, with the help of approximate renormalization group methods, the universal behavior of polymer solutions undergoing shear flow. The solvent quality crossover scaling behavior of viscometric functions was, however, not reported by these authors. Recently, Prakash[17,19] has obtained, with the help of a Gaussian approximation, universal material functions in shear flow, both in the crossover regime and in the excluded volume limit.

A systematic methodology by which it is possible to go beyond approximate results, and obtain exact results (albeit within numerical error bars) of the influence of solvent quality, in terms of the parameter z, on both

equilibrium and non-equilibrium properties, has been newly introduced by Kumar and Prakash.[24] Basically, they showed that model independent predictions can be obtained by extrapolating *exact*[42] Brownian dynamics simulations data, acquired for chains of finite length, to the limit of infinite chain length. While their methodology is applicable to both regimes of behavior, they restricted their attention to the prediction of equilibrium and linear viscoelastic properties. In this paper, we apply their procedure and obtain, for the first time, *exact* predictions of the universal crossover dependence of viscometric functions on z, at various values of the characteristic non-dimensional shear rate, $\beta = \lambda_{\mathrm{p}} \dot{\gamma}$, where λ_{p} is a characteristic relaxation time defined by,

$$\lambda_{\mathrm{p}} = \frac{[\eta]_0 M \eta_{\mathrm{s}}}{N_{\mathrm{A}} k_{\mathrm{B}} T} \qquad (1)$$

Here, k_{B} is Boltzmann's constant, η_{s} is the solvent viscosity, $[\eta]_0$ is the zero shear rate intrinsic viscosity, and N_{A} is Avogadro's number. The same methodology is also used here to calculate the dependence of several properties on β, in the excluded volume limit. This includes, for instance, the power-law scaling of viscometric functions with β for large values of β, and the dependence of the orientation of the polymer coil with respect to the flow direction, on the magnitude of β. The important question of whether the value of the critical exponent ν (which governs the scaling of the mean size of a polymer chain with molecular weight in the long chain limit), is unaltered in shear flow, is also addressed here within this framework.

In addition to excluded volume interactions, it is now well established that it is also essential to include solvent mediated hydrodynamic interactions between different segments of a polymer chain, in order to obtain an accurate description of the universal dynamics of polymer solutions. While several studies (based on bead-spring chain models) of the combined influence of excluded volume, hydrodynamic interaction, and even finite extensibility effects, on rheological properties have been reported so far, they have generally been restricted to finite chains.[16,21,22,25,26] However, Zylka and Öttinger[10] have examined the universal consequences of the presence of both excluded volume and hydrodynamic interaction effects on properties far from equilibrium, with the help of approximate renormalization group methods. Several important advances in recent years, within the framework of Brownian dynamics simulations, have now made it feasible to treat hydrodynamic interaction effects, free of any simplifying approximations, in bead-spring chain models with a large number of beads.[27,28] In this work, however, we confine attention to excluded volume interactions alone, for two reasons. First, we wish to examine, in isolation, the influence of excluded volume interactions on long chain properties, before considering the more complex possibilities that arise in the presence of other non-linearities. The preliminary results of Prabhakar and Prakash,[21] who show that in fact the various

non-linearities appear to be decoupled from each other, suggests that there is some value in looking at these effects in isolation from each other. Second, and more practically, the procedure adopted here of extrapolating finite chain simulation data to the long chain limit becomes significantly more computationally intensive when both excluded volume and hydrodynamic interactions are included. The results of the present paper are therefore not yet directly comparable with experiments. Nevertheless, while the more ambitious task of a complete description of polymer solution dynamics is being simultaneously pursued, it is felt that several important conclusions with regard to the role of solvent quality, can still be made within the present approach.

The plan of the paper is as follows. In sec. II, we state the governing equations, define the various properties calculated in this work, and summarize the previously introduced procedure for obtaining *exact* predictions of properties in the crossover regime and in the excluded volume limit. In sec. III A, asymptotic results describing the dependence of the normalized viscosity and the normalized first normal stress difference on β and z, are presented. The excluded volume limit dependence on β, of various properties, is discussed in sec. III B, along with a comparison with results obtained previously with the Gaussian approximation. Finally, the principal conclusions of this work are summarized in sec. IV.

II. BEAD-SPRING CHAINS WITH EXCLUDED VOLUME INTERACTIONS

A. Governing equations

Within the framework of a numerical solution strategy, the most appropriate model for the task of describing the rheological behavior of dilute polymer solutions, in the limit of long chains, is a bead-spring chain model. The internal configuration of a bead-spring chain, suspended in a Newtonian solvent undergoing homogeneous flow, with the beads located at positions $\boldsymbol{r}_{\nu}$, $\nu = 1, \ldots, N$ with respect to an arbitrarily chosen origin, can be specified by the $N-1$ bead connector vectors, $\boldsymbol{Q}_k = \boldsymbol{r}_{k+1} - \boldsymbol{r}_k$, $k = 1, \ldots, N-1$, connecting beads k and $k+1$. For Hookean springs, and a pairwise intra-molecular excluded volume force, the potential energy of a bead-spring chain is given by the expression,

$$\phi = \frac{1}{2} H \sum_{i=1}^{N-1} \boldsymbol{Q}_i \cdot \boldsymbol{Q}_i + \frac{1}{2} \sum_{\substack{\nu, \, \mu=1 \\ \nu \neq \mu}}^{N} E\left(\boldsymbol{r}_{\nu} - \boldsymbol{r}_{\mu}\right) \qquad (2)$$

where, H is the spring constant, and $E\left(\boldsymbol{r}_{\nu} - \boldsymbol{r}_{\mu}\right)$ is the excluded volume potential between the beads ν and μ of the chain. The key ingredient, in the procedure for obtaining universal predictions in terms of the parameter z, is the use of the narrow Gaussian potential to represent

excluded volume interactions,

$$E\left(\boldsymbol{r}_\nu - \boldsymbol{r}_\mu\right) = \left(\frac{z^*}{d^{*3}}\right) k_{\mathrm{B}}T \exp\left\{-\frac{H}{2k_{\mathrm{B}}T}\frac{r_{\nu\mu}^2}{d^{*2}}\right\} \quad (3)$$

where, $\boldsymbol{r}_{\nu\mu} = \boldsymbol{r}_\nu - \boldsymbol{r}_\mu$, is the vector between beads μ and ν, the nondimensional parameter z^*, as mentioned previously, measures the strength of the excluded volume interaction, and d^* is a measure of the range of excluded volume interaction. Prakash and coworkers have shown, in their examination of universal linear viscoelastic and steady shear flow properties in the context of the Gaussian approximation,[17,19] and in their calculation of universal equilibrium and linear viscoelastic properties with Brownian dynamics simulations,[24] that the usefulness of the narrow Gaussian potential stems from the fact that, as $N \to \infty$, (i) the parameters z^* and N combine together to form the single variable, $z = z^*\sqrt{N}$, and (ii) the choice of d^* is inconsequential because the parameter d^* always appears in the theory as the re-scaled variable $d^*/\sqrt{N}$. These results form the basis of our exploration, in this work, of the universal behavior of bead-spring chains subject to shear flow.

As will be discussed in greater detail shortly in sec. II B below, all properties of interest in the present work can be calculated from appropriately defined configurational averages. Unfortunately, it is currently infeasible to solve the nonlinear diffusion equation that governs the time evolution of the configurational distribution function in the presence of excluded volume interactions. However, configurational averages can be numerically evaluated directly from ensembles of polymer configurations. Basically, stochastic trajectories that describe the temporal evolution of an ensemble of chain configurations can be generated by solving the stochastic differential equation that governs the bead connector vectors, with the help of Brownian dynamics simulations.[29] In terms of the nondimensional variables,

$$\boldsymbol{Q}_k^* = \frac{1}{\ell}\,\boldsymbol{Q}_k;\ \ t^* = \frac{t}{\lambda_H};\ \ \phi^* = \frac{\phi}{k_B T};\ \ \boldsymbol{\kappa}^* = \lambda_H \boldsymbol{\kappa} \quad (4)$$

where, $\ell = \sqrt{k_{\mathrm{B}}T/H}$ is a length scale that is proportional to the root mean square extension of a single spring in the Rouse model, $\lambda_H = \zeta/4H$ is a time constant (with ζ representing the bead friction coefficient), and $\boldsymbol{\kappa}(t)$ is the traceless transpose of the velocity-gradient tensor for the homogeneous flow field (which can be a function of time but is independent of position), the stochastic differential equation that governs the trajectories of the bead connector vectors in the presence of excluded volume interactions, is given by the expression,[19]

$$d\boldsymbol{Q}_j^* = \left[\boldsymbol{\kappa}^* \cdot \boldsymbol{Q}_j^* - \frac{1}{4}\sum_{k=1}^{N-1} A_{jk}\frac{\partial\phi^*}{\partial\boldsymbol{Q}_k^*}\right]dt^* + \sqrt{\frac{1}{2}}\sum_{\nu-1}^{N}\bar{B}_{j\nu}\,d\boldsymbol{W}_\nu^*$$
$$(5)$$

Here, $\boldsymbol{W}_\nu^*$ is a Wiener process, whose $3N$−dimensional

components satisfy,

$$\langle W_{\nu,j}^*(t^*)\rangle = 0$$
$$\langle W_{\nu,j}^*(t^*)W_{\mu,k}^*(t^{*\prime})\rangle = \min(t^*, t^{*\prime})\delta_{jk}\delta_{\nu\mu} \quad (6)$$

for $j, k = 1, 2, 3$ and $\nu, \mu = 1, 2, 3, \ldots, N$. The quantity $\overline{B}_{k\nu}$ is an $(N-1) \times N$ matrix defined by, $\overline{B}_{k\nu} = \delta_{k+1,\,\nu} - \delta_{k\nu}$, with $\delta_{k\nu}$ denoting the Kronecker delta, and A_{jk} is the Rouse matrix,

$$A_{jk} = \sum_{\nu=1}^{N} \overline{B}_{j\nu}\overline{B}_{k\nu} = \begin{cases} 2 & \text{for } |j-k| = 0, \\ -1 & \text{for } |j-k| = 1, \\ 0 & \text{otherwise} \end{cases} \quad (7)$$

Before discussing the two different simulation schemes used here for solving Eq. (5) to obtain predictions of the universal crossover and excluded volume limit behaviors, it is appropriate to first introduce all the properties, and their defining equations, that are calculated in the present work.

B. Material functions

We confine our attention in this work to steady simple shear flows, which are specified by the following matrix representation for the tensor $\boldsymbol{\kappa}$ in a laboratory-fixed coordinate system,

$$\boldsymbol{\kappa} = \dot{\gamma}\begin{pmatrix} 0 & 1 & 0 \\ 0 & 0 & 0 \\ 0 & 0 & 0 \end{pmatrix} \quad (8)$$

where, $\dot{\gamma}$ is the constant shear rate.

The principle material functions of interest here are the polymer contribution to the viscosity, η_{p}, and the first normal stress difference, Ψ_1. Since hydrodynamic interactions have not been included in the present model, the second normal stress difference is identically zero.[30] In terms of the components of the polymer contribution to the stress tensor, $\tau_{xy}^{\mathrm{P}}, \tau_{xx}^{\mathrm{P}}$, etc, η_{p}, and Ψ_1, can be obtained from the following relations,[31]

$$\tau_{xy}^{\mathrm{P}} = -\dot{\gamma}\,\eta_{\mathrm{p}};\qquad \tau_{xx}^{\mathrm{P}} - \tau_{yy}^{\mathrm{P}} = -\dot{\gamma}^2\,\Psi_1 \quad (9)$$

Within the framework of polymer kinetic theory, the polymer contribution to the stress tensor, $\boldsymbol{\tau}^{\mathrm{P}}$, can be calculated by either the *Kramers* or the *Giesekus* expressions. While the latter expression becomes invalid in the presence of hydrodynamic interactions, it has been shown to remain valid in the presence of excluded volume interactions.[18] The relative magnitude of the variance associated with the use of either of these expressions in Brownian dynamics simulations has been examined previously by Prakash[19] and it has been shown that the Giesekus expression always leads, particularly at low shear rates, to a smaller value of variance. For this reason, we have

used the Giesekus expression in our work, which at steady state has the form,

$$\boldsymbol{\tau}^{\mathrm{P}} = -\frac{n_{\mathrm{p}}\zeta}{2}\sum_{m,n=1}^{N-1} C_{mn}\left\{\boldsymbol{\kappa}\cdot\langle\boldsymbol{Q}_m\boldsymbol{Q}_n\rangle + \langle\boldsymbol{Q}_m\boldsymbol{Q}_n\rangle\cdot\boldsymbol{\kappa}^T\right\} \tag{10}$$

where, C_{mn} is the Kramers matrix. The Kramers matrix is the inverse of the Rouse matrix, and is defined by,

$$C_{mn} = \sum_{\nu=1}^{N} B_{\nu m}B_{\nu n} = \min(m,n) - \frac{m\,n}{N} \tag{11}$$

Here, the $N\times(N-1)$ matrix $B_{\nu k}$ is defined by, $B_{\nu k} = k/N - \Theta(k-\nu)$, with $\Theta(k-\nu)$ denoting a Heaviside step function. As will be discussed in greater detail in sec. II C below, we further reduce the variance in our simulations by implementing a variance reduction procedure based on the method of control variates.[29]

In the limit of zero shear rate, the ratio $U_{\Psi\eta}$, which is defined by the expression,

$$U_{\Psi\eta} = \frac{n_p\,k_BT\Psi_1}{\eta_p^2} \tag{12}$$

where, n_p is the number density of polymers, has been shown to have a universal value, both in theta solutions,[29] and in good solvents.[24] In the context of a dumbbell model, Prakash and Öttinger[13] have evaluated its dependence on the non-dimensional shear rate $\lambda_H\dot{\gamma}$. In this work, we seek to examine the universal dependence of $U_{\Psi\eta}$ on the characteristic shear rate β, in the excluded volume limit.

In addition to rheological properties, it is also of interest to examine the *anisotropy* induced in any arbitrary tensorial property of the solution, due to the orientation and deformation of polymer coils caused by the flow field. The precise definition of anisotropy is taken up shortly below. Of particular relevance in this work, is the change in the degree of anisotropy brought about by the presence of excluded volume interactions.

In order to obtain an estimate of the anisotropy of any tensorial quantity $\boldsymbol{\sigma}$, we begin by noting that in simple shear flows $\boldsymbol{\sigma}$ must reflect the symmetry of the flow field. In particular, since shear flows are invariant when the direction of the z-axis is reversed,[31] the xz, yz, zx and zy components of $\boldsymbol{\sigma}$ must be zero. As a result, $\boldsymbol{\sigma}$ must have the following matrix representation in the laboratory-fixed coordinate system,

$$\boldsymbol{\sigma} = \begin{pmatrix} \sigma_{xx} & \sigma_{xy} & 0 \\ \sigma_{yx} & \sigma_{yy} & 0 \\ 0 & 0 & \sigma_{zz} \end{pmatrix} \tag{13}$$

It is clear from Eq. (13) that the z-axis is a principal direction. It follows that the other two principal directions must lie in the xy plane. We denote the principal axes in this plane by $\bar{x}$ and $\bar{y}$, with the $\bar{x}$ axis making an angle χ_σ

with the x-axis. Thus by rotating the coordinate system by χ_σ, the matrix that represents $\boldsymbol{\sigma}$ can be diagonalized. By exploiting the rules for change of tensor components, the orientation of the (x,y,z) coordinate system relative to the $(\bar{x},\bar{y},\bar{z})$ coordinate system can be calculated to be,

$$\tan 2\chi_\sigma = \frac{2\sigma_{xy}}{\sigma_{xx}-\sigma_{yy}} \tag{14}$$

With the help of symmetry arguments, one can show that the orientation angle $\chi_\sigma = \pi/4$ close to equilibrium. As the shear rate increases, χ_σ is expected to decrease to zero, reflecting the increasing alignment of the polymer coils with the flow direction. The orientation angle χ_σ, therefore, serves as a measure of the anisotropy of $\boldsymbol{\sigma}$.[15]

It is straightforward to show that the orientation angle associated with the polymer contribution to the stress tensor, χ_τ, is given by,[15,32]

$$\tan 2\chi_\tau = \frac{2\tau_{xy}^{\mathrm{P}}}{\tau_{xx}^{\mathrm{P}}-\tau_{yy}^{\mathrm{P}}} = \frac{m_\tau}{\beta} \tag{15}$$

where the quantity m_τ, defined by the above expression, is frequently referred to as the *orientation resistance*.[32] In the Rouse model, m_τ is a constant, independent of the shear rate, with a value 2.5. In a similar manner, the orientation angle associated with the radius of gyration tensor, $\boldsymbol{G}$, is given by the expression,[15,32]

$$\tan 2\chi_G = \frac{2G_{xy}}{G_{xx}-G_{yy}} = \frac{m_G}{\beta} \tag{16}$$

where, m_G is the corresponding orientation resistance, and G_{xy} etc., represent components of the tensor $\boldsymbol{G}$, defined by,

$$\boldsymbol{G} = \frac{1}{N}\sum_{\nu=1}^{N}\langle(\boldsymbol{r}_\nu-\boldsymbol{r}_c)(\boldsymbol{r}_\nu-\boldsymbol{r}_c)\rangle \tag{17}$$

Here, $\boldsymbol{r}_c$ denotes the position of the center of mass. In the Rouse model, $m_G = 1.75$. It is worthwhile noting that while the orientation of the macromolecule measured by flow birefringence coincides with χ_τ (according to the "stress optical" law), χ_G is the orientation angle measured by static light scattering.[32] In this work, we show that in the presence of excluded volume interactions, both m_τ and m_G are not constant, but rather are functions of the characteristic shear rate β, and we examine this dependence in the excluded volume limit.

C. Simulation schemes

Two different simulation schemes have been introduced and discussed in detail by Prakash and co-workers in order to find the universal properties of polymer solutions in the crossover region, and in the excluded volume limit, respectively.[19,24] Here, we summarize them briefly.

The universal dependence of various properties on the parameter z in the long chain limit is found by a two step procedure: (i) Simulations are carried out for increasing values of N, keeping the value of z ($= z^* \sqrt{N}$), constant, and (ii) The accumulated finite chain data for any property is then extrapolated to the limit $N \to \infty$. The crossover behavior of the property is obtained by repeating steps (i) and (ii) for a number of values of z. In the Gaussian approximation, the value of the parameter d^* was held constant during the process of accumulating finite chain data,[17,19] and it was shown that the particular choice of value for d^* was inconsequential in the limit $N \to \infty$. On the other hand, while obtaining the crossover behavior of equilibrium and linear viscoelastic properties with Brownian dynamics simulations,[24] the parameter d^* was chosen such that,

$$d^* = k \, (z^*)^{1/5} \tag{18}$$

where, k is an arbitrary constant. Note that, for a fixed value of z, since $z^* \to 0$ (or equivalently, $T \to T_\theta$), as $N \to \infty$, this choice of d^* implies that the asymptotic limit is reached along trajectories in the (z^*, d^*) parameter space that converge to the origin. It was shown by Kumar and Prakash[24] that choosing d^* values according to Eq. (18), permits the use of larger step sizes in the numerical integration scheme. The independence of the asymptotic results from the particular choice of k (and consequently the trajectory in the (z^*, d^*) parameter space), was also established in ref. 24. Since Brownian dynamics simulations are used in the present work to obtain the crossover behavior, d^* values will be chosen according to Eq. (18).

Universal properties in the excluded volume limit ($z \to \infty$) are obtained by accumulating finite chain data for constant values of z^* (which is equivalent to the temperature T being constant), followed by extrapolation to the infinite chain length limit. Since for any constant value of z^*, $z \to \infty$, as $N \to \infty$, we expect that properties obtained in the excluded volume limit will be independent of the particular choice of z^*. Prakash and co-workers[19,24] have shown that this is indeed the case, for the situations examined previously by them. As will be discussed in greater detail subsequently, this independence will be used in the present work to indicate the adequacy or otherwise of the accumulated finite chain data.

The various configurational averages required to calculate the properties listed in sec. II B above were obtained with a second order predictor-corrector Brownian dynamics simulation algorithm originally proposed by Iniesta and Garcia de la Torre.[33] A detailed discussion of the algorithm, adapted for the problem at hand, can be found in ref. 19. In a typical simulation, roughly 80,000 trajectories, with Gaussian initial distributions, were generated, and the integration was carried out until a stationary state was attained. Message Passing Interface (MPI) clusters were used to distribute the trajectories across several processors. Since the present algorithm belongs to the class of embarrassingly parallel algorithms, the wall time scales with the number of processors used. Typically, three different time steps $\Delta t^* = 1.0, \, 0.6, \, \text{and} \, 0.5$ were used, and the results were then extrapolated to zero time step using the subroutine TEXTRA suggested by Öttinger[29]. This extrapolation procedure enabled the simulations to be carried out at relatively large time steps.

A key ingredient in the simulation strategy adopted here, as mentioned perviously, is the use of a variance reduction procedure based on the method of control variates, in order to reduce the statistical error in the simulations. This is crucial because the magnitude of the error in the finite chain data significantly affects the accuracy of the extrapolation to the infinite chain length limit. Since a fairly involved discussion of the procedure has been given previously in ref. 24, it is not repeated here. However, a few salient features are highlighted below.

The essence of the scheme (and the vital factor that decides its success or otherwise) is to find a control variable whose mean value is known exactly, and whose fluctuations are correlated with the variable whose variance we are interested in reducing. It was found by Kumar and Prakash,[24] that the Rouse model serves as an excellent source of control variables for all the equilibrium and linear viscoelastic properties that were evaluated by them. In this work, we have again used the Rouse model as the source of control variables, and found that as before, this leads to a significant reduction in the variance of all properties. At first sight, this result is somewhat surprising. In the case of equilibrium and linear viscoelastic properties, since only equilibrium averages were evaluated, both the stochastic differential equation, Eq. 5, and the stochastic differential equation in the Rouse model, were solved with the term involving κ set equal to zero. In the present instance, since we are interested in properties at finite shear rates, both equations were integrated with the κ term in place. In spite of including this term in the Rouse model, as is well known, viscometric functions predicted by it are constant and independent of shear rate. This is not the case, however, in the presence of excluded volume interactions, where, as we shall see shortly, viscometric functions decrease with an increase in shear rate. The success in the variance reduction strategy suggests, therefore, that even though the Rouse viscometric functions are independent of shear rate, the fluctuations in the Rouse control variables remain correlated with their corresponding variables in the presence of excluded volume interactions. The reason for this occurance might lie in the fact that with increasing shear rate, the beads of the chain are drawn further apart, and the resultant weakening of the excluded volume interactions actually brings the results of the two models closer together.

III.   UNIVERSAL PROPERTIES

A.   Crossover behavior

In this subsection, we are concerned with obtaining the crossover behavior of the universal ratios, $\eta_p/\eta_{p,0}$, and $\Psi_1/\Psi_{1,0}$ (where, $\eta_{p,0}$ and $\Psi_{1,0}$ are the zero shear rate polymer contributions to the viscosity and first normal stress difference, respectively), as a function of the characteristic shear rate β, using the simulation scheme described in sec. II C above. A strict pursuance of this procedure would require the construction of each of these ratios at various values of N, using equilibrium simulations (as described previously in ref. 24) to find $\eta_{p,0}$ and $\Psi_{1,0}$, and simulations at finite shear rates (as described above) to find η_p and Ψ_1, followed by extrapolation to the long chain limit. Unfortunately, this procedure suffers from a serious problem. Since both the denominator and the numerator are found by Brownian dynamics simulations, the ratios have relatively large statistical error bars, which makes their extrapolation to the $N \to \infty$ limit highly inaccurate. Fortunately, this difficulty can be overcome by adopting the following procedure.

We first note that,

$$\lim_{N \to \infty} \frac{\eta_p}{\eta_{p,0}} = \frac{\lim_{N \to \infty}(\eta_p/\eta_p^R)}{\lim_{N \to \infty}(\eta_{p,0}/\eta_p^R)} \tag{19}$$

$$\lim_{N \to \infty} \frac{\Psi_1}{\Psi_{1,0}} = \frac{\lim_{N \to \infty}(\Psi_1/\Psi_1^R)}{\lim_{N \to \infty}(\Psi_{1,0}/\Psi_1^R)} \tag{20}$$

where, η_p^R and Ψ_1^R are the viscosity and first normal stress difference predicted by the Rouse model, respectively,[30]

$$\eta_p^R = n_p \lambda_H k_B T \left[\frac{(N^2 - 1)}{3} \right] \tag{21}$$

$$\Psi_1^R = 2 n_p \lambda_H^2 k_B T \left[\frac{(N^2 - 1)(2N^2 + 7)}{45} \right] \tag{22}$$

Kumar and Prakash have previously evaluated the ratios $\eta_{p,0}/\eta_p^R$ and $\Psi_{1,0}/\Psi_1^R$ in the long chain limit.[24] For the purpose of evaluating $\eta_p/\eta_{p,0}$ in the long chain limit, therefore, it suffices to evaluate the ratios, η_p/η_p^R and Ψ_1/Ψ_1^R, as $N \to \infty$. The simulation scheme described in sec. II C above has, consequently, been used here to evaluate these ratios at various values of z.

Figures 1 clearly indicate the independence of the extrapolated values of η_p/η_p^R and Ψ_1/Ψ_1^R, in the $N \to \infty$ limit, from the trajectories in the (z^*, d^*) parameter space used to obtain them. The parameters z and β have been held constant at a value of unity, while carrying out simulations at increasing values of N, for three different values of k. In each simulation, $z^* = z/\sqrt{N}$, while d^* is found from eq 18. In order to keep β constant in each simulation, the non-dimensional shear rate $\lambda_H \dot{\gamma}$ used in the simulation, at each value of N, has been calculated from the expression, $\lambda_H \dot{\gamma} = \beta (\lambda_H n_p k_B T/\eta_{p,0})$, which can be derived from Eq. 1 for a dilute polymer solution.
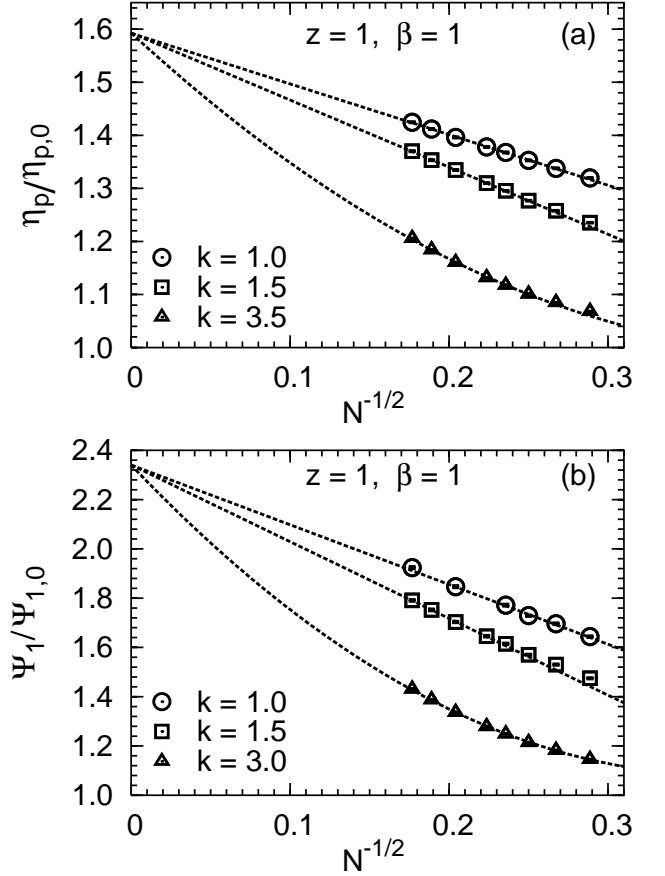

FIG. 1: (a) The ratio of the viscosity to the Rouse model viscosity, and (b) The ratio of the first normal stress difference to the Rouse model first normal stress difference, versus $1/\sqrt{N}$ at $z = 1$ and $\beta = 1$, for three different values of k. The symbols, with error bars, represent the simulation results, while the lines are least-square curve fits to the data.

As mentioned earlier, $(\eta_{p,0}/\lambda_H n_p k_B T)$ can be evaluated by carrying out equilibrium simulations for the same set of parameter values as those used in the finite shear rate simulations. Extrapolation of the finite chain data has been carried out by plotting simulation results versus $1/\sqrt{N}$, since Prakash[18] has shown previously that leading order corrections to the infinite chain length limit, of various material properties, are of order $1/\sqrt{N}$. Furthermore, as mentioned earlier, the parameter d^* always occurs in the theory as the ratio $d^*/\sqrt{N}$. The asymptotic values obtained in this manner correspond to the viscosity and first normal stress difference ratios for a δ-function excluded volume potential, at $z = 1$ and $\beta = 1$. The same procedure was then repeated for various values of z and β.

The universal dependence of $\eta_p/\eta_{p,0}$, and $\Psi_1/\Psi_{1,0}$ on β, at various values of z, obtained by combining the infinite chain length results for the ratios η_p/η_p^R and Ψ_1/Ψ_1^R, with the infinite chain length zero shear rate ratios evaluated previously by Kumar and Prakash,[24] are presented
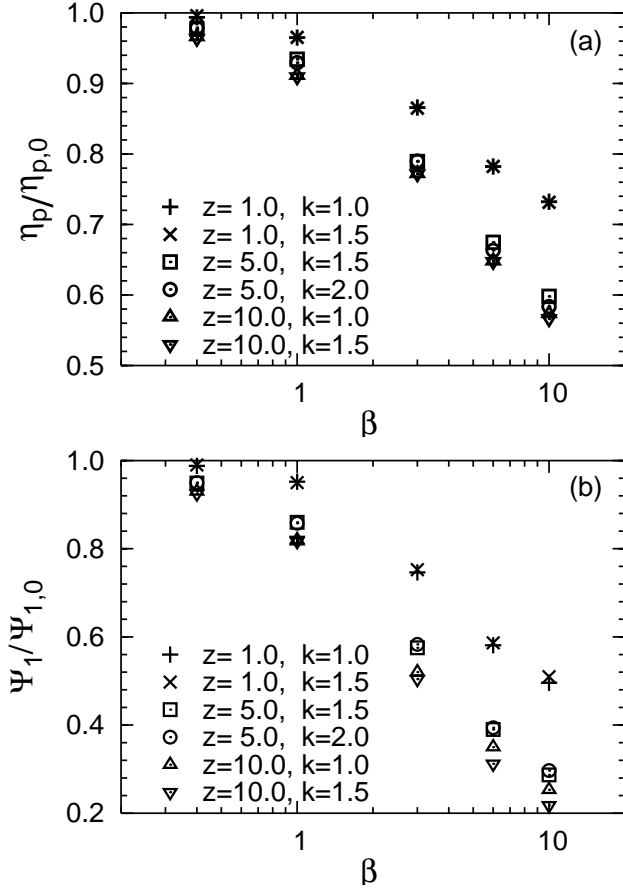
FIG. 2: (a) Asymptotic nondimensional viscosity ratio ($\eta_p/\eta_{p,0}$), and (b) Asymptotic nondimensional first normal stress difference ratio ($\Psi_1/\Psi_{1,0}$), versus the characteristic shear rate β, for various values of z and k
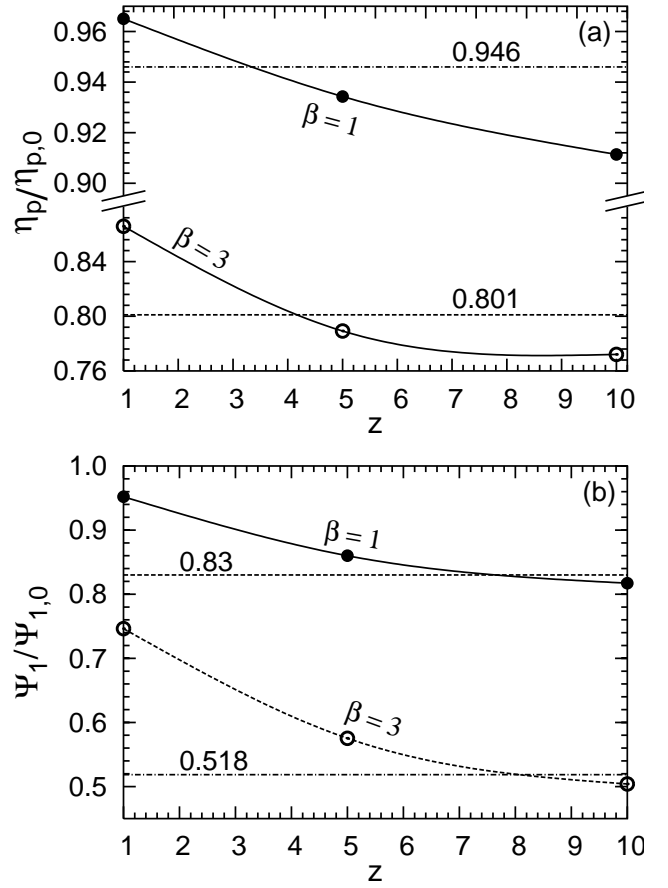

FIG. 3: (a) Asymptotic non-dimensional viscosity ratio ($\eta_p/\eta_{p,0}$), and (b) Asymptotic non-dimensional first normal stress difference ratio ($\Psi_1/\Psi_{1,0}$), plotted against z for two different values of β. Symbols denote values obtained in the crossover regime, while the horizontal lines correspond to values of the ratios in the excluded volume limit.

in Figs. 2. At each value of z, extrapolated data for two different values of k are displayed in order to clearly delineate the limit of β up to which the current asymptotic results are valid. In essence, beyond some threshold value of the characteristic shear rate, say $\beta^\dagger$, the lack of coincidence of data for two different values of k, implies that the present finite chain data, accumulated for chains with $N \leq 36$, is no longer sufficient to obtain an accurate extrapolation. For $\beta > \beta^\dagger$, the flow field begins to probe model dependent length scales, and scale invariance, which is responsible for the observed model independence, no longer exists. The results in Figs. 2 suggest that $\beta^\dagger$ for $\Psi_1/\Psi_{1,0}$ is smaller than that for $\eta_p/\eta_{p,0}$, and in both cases, it decreases with increasing z.

It is clear from Figs. 2 that the presence of excluded volume interactions leads to shear thinning, and that the extent of shear thinning increases with increasing solvent quality. However, the incremental increase in shear thinning with increasing values of z, for a given value of β, appears to decrease as z increases. This can be seen more clearly from Figs. 3, where the asymptotic viscometric ratios are plotted versus the solvent quality z, at

two representative values of β. In each case, the ratios decrease, but with decreasing rate, as the solvent quality increases, before appearing to level off at a final solvent quality independent value, in the limit of large z. In this excluded volume limit, consequently, universal viscometric functions would depend only on β, and on no other parameter.

It is not possible here to explore further the approach of the crossover regime to the excluded volume limit, because the present finite chain data is not sufficient to obtain accurate extrapolations. Obtaining such data is, unfortunately, currently prohibitively expensive computationally. Nevertheless, behavior in the excluded volume limit itself can be directly obtained, as has been discussed earlier. The horizontal lines in Figs. 3 correspond to excluded volume limit values of the viscometric ratios obtained by these means, the details of which will be described in greater detail shortly. It is immediately apparent that the large z asymptote of the crossover regime does not coincide with the excluded volume limit.
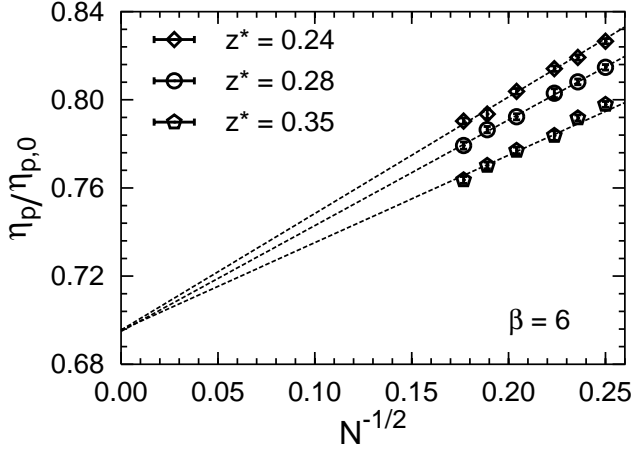
FIG. 4: Non-dimensional viscosity ratio $\eta_p/\eta_{p,0}$, plotted against $1/\sqrt{N}$, for three different values of z^*, and for $\beta = 6$. Symbols are predictions of Brownian dynamics simulations, while lines are least square curve fits through the data.

This is in complete contrast to the universal results, in steady shear flow, obtained earlier by Prakash[19] with the Gaussian approximation. While the general behavior in the crossover regime predicted by the Gaussian approximation is identical to that described above, values of viscometric ratios for $z \gg 1$ were found to smoothly approach those obtained in the excluded volume limit. This perplexing behavior, where predictions of the Gaussian approximation differ qualitatively from those of *exact* Brownian dynamics simulations, was also observed recently by Kumar and Prakash in their attempt to predict the behavior of universal equilibrium and linear viscoelastic ratios.[24] Before discussing the origins of this behavior in greater detail, however, it is necessary to complete the presentation of a few further results obtained in the excluded volume limit.

B. Excluded volume limit

Predictions in the excluded volume limit are obtained, as described in sec. II C above, by extrapolating finite chain data acquired for various constant values of z^*, to the infinite chain length limit. Figure 4 is an illustrative example, where simulations have been carried out at several values of N, for $z^* = 0.24, 0.28$, and 0.35, respectively, and at a fixed value of $\beta = 6$, in order to acquire data for the ratio $\eta_p/\eta_{p,0}$. The common extrapolated value, in the limit $N \to \infty$, for all the three values of z^*, is the universal value, in the excluded volume limit, of $\eta_p/\eta_{p,0}$, at $\beta = 6$. As in the case of extrapolated values in the crossover regime, insufficiency in the accumulated finite chain data is revealed when curves for different values of z^* fail to extrapolate to a common point. In the present instance, this typically occurs for values of characteristic shear rate $\beta \gtrsim 10$. Extrapolated data obtained in this manner, at various values of β (up to $\beta \approx 10$),
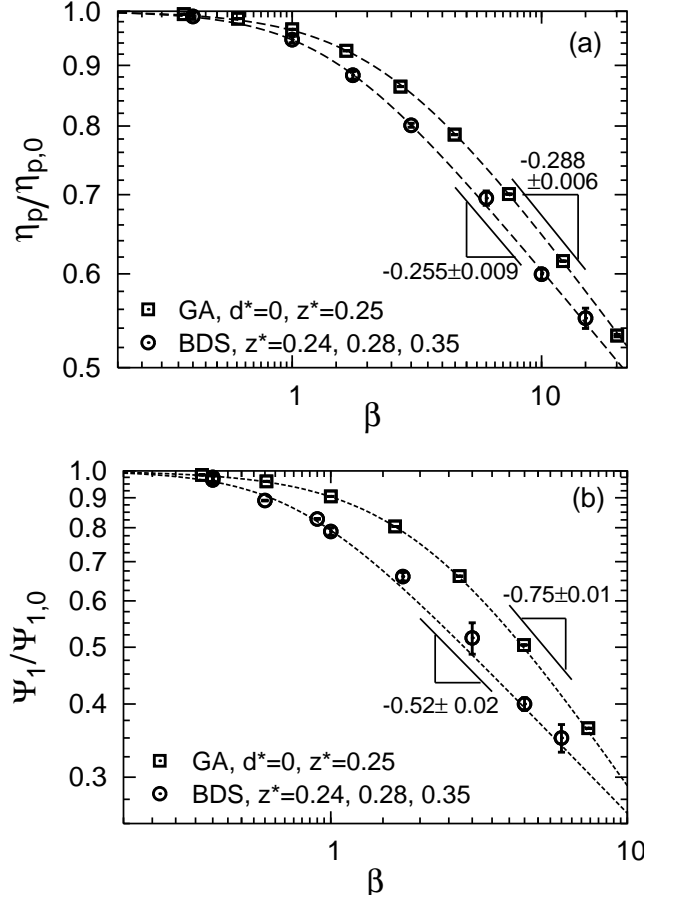

FIG. 5: (a) Asymptotic non-dimensional ratio $\eta_p/\eta_{p,0}$, and (b) Asymptotic nondimensional ratio $\Psi_1/\Psi_{1,0}$, for various values of β, in the excluded volume limit. Circles represent Brownian dynamics simulation data, while squares represent results of the Gaussian approximation. The dashed lines are fits to the data using the Carreau-Yasuda model, Eqs. (23).

for both the viscometric ratios, are displayed in Figs. 5. The horizontal lines, displayed in Figs. 3 earlier, have also been obtained similarly.

Both the viscometric functions displayed in Figs. 5 exhibit a similar dependence on β—nearly constant values at small values of β, followed by a crossover to a power law dependence at large values of β. Results obtained earlier with the Gaussian approximation are also presented in Figs. 5 for comparison. While the extent of shear thinning is under-predicted by the Gaussian approximation for the values of β displayed in the figures, it predicts a larger slope in the power law regime, which implies that the shear thinning predicted by it will eventually be greater than *exact* Brownian dynamics simulations.

The Carreau-Yasuda model, which proposes the following expressions for describing the variation of the vis-

TABLE I: Values of Carreau-Yasuda model parameters for $\eta_p/\eta_{p,0}$ and $\Psi_1/\Psi_{1,0}$. Comparison of exact Brownian dynamics simulations (BDS), with the Gaussian approximation (GA).

	m_η	n_η	a_η
BDS	-0.255 ± 0.009	1.925 ± 0.100	0.712 ± 0.050
GA	-0.288 ± 0.006	1.675 ± 0.097	0.429 ± 0.025
	m_ψ	n_ψ	a_ψ
BDS	-0.52 ± 0.02	2.395 ± 0.090	1.312 ± 0.020
GA	-0.750 ± 0.014	1.878 ± 0.795	0.507 ± 0.012

cometric ratios with β,

$$
\frac{\eta_{\mathrm{P}}}{\eta_{\mathrm{p,0}}} = [1 + (a_\eta\,\beta)^{n_\eta}]^{\frac{m_\eta}{n_\eta}} \; ; \quad \frac{\Psi_1}{\Psi_{1,0}} = [1 + (a_\psi\,\beta)^{n_\psi}]^{\frac{m_\psi}{n_\psi}}
$$
(23)

has been shown previously by Prakash[19] to provide a good fit to the results of the Gaussian approximation. As indicated in Figs. 5, with a suitable choice of the fitting coefficients a_η, m_η, n_η etc., it also leads to a good fit of Brownian dynamics simulation data. The values of the fitting coefficients used in the two cases are displayed in Table I. The constant m represents the slope of the power law region at large values of β. In line with the expectation by visual inspection, the value of m for the Gaussian approximation is larger than that for *exact* Brownian dynamics simulations. Using renormalization group methods, Öttinger[9,23] has previously found that the values, $m_\eta = -0.25$ and $m_\psi = -0.5$, describe the power law shear rate dependence of $\eta_p/\eta_{p,0}$, and $\Psi_1/\Psi_{1,0}$, respectively, in the excluded volume limit. As is evident from the values of the power law exponents displayed in Table I, the predictions of Brownian dynamics simulations are in remarkable agreement with renormalization group results.

The expression for $U_{\Psi\eta}$, Eq. (12), can be rewritten in the form,

$$
U_{\Psi\eta} = U_{\Psi\eta,0}\,\frac{(\Psi_1/\Psi_{1,0})}{(\eta_p/\eta_{p,0})^2}
$$
(24)

$$
= U_{\Psi\eta,0}\,\frac{[1 + (a_\psi\beta)^{n_\psi}]^{(m_\psi/n_\psi)}}{[1 + (a_\eta\beta)^{n_\eta}]^{(2m_\eta/n_\eta)}}
$$
(25)

where, $U_{\Psi\eta,0}$ is the value of $U_{\Psi\eta}$ in the zero shear rate limit, and the Carreau-Yasuda model expression, Eq. (23), has been used for the viscometric ratios. Both renormalization group results, and the present Brownian dynamics simulations suggest that, $m_\psi \approx 2m_\eta \approx -0.5$ (see Table I). For $\beta \gg 1$, therefore, Eq. (25) can be simplified to,

$$
U_{\Psi\eta} = U_{\Psi\eta,0}\,\sqrt{\frac{a_\eta}{a_\psi}}
$$
(26)

Kumar and Prakash[24] have estimated that in the excluded volume limit, $U_{\Psi\eta,0} = 0.771 \pm 0.009$. Substituting
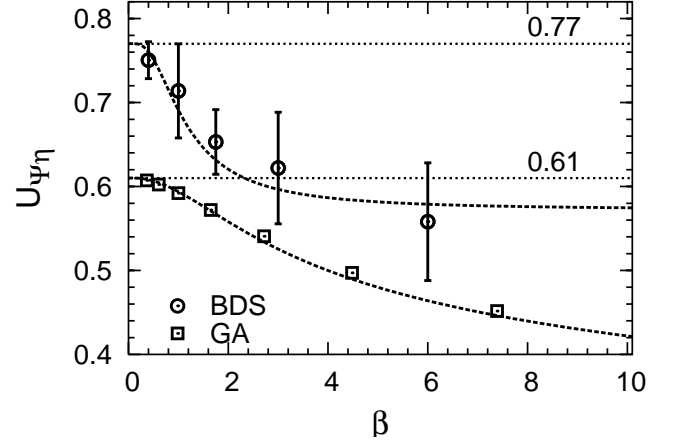

FIG. 6: The dependence of the universal ratio $U_{\Psi\eta}$ on the characteristic shear rate β. The open circles are predictions of Brownian dynamics simulations, while the squares are predictions of the Gaussian approximation, calculated from data reported by Prakash.[18] The dashed curves have been obtained from Eq. (25), using values for the Carreau-Yasuda model parameters given in Table I. The horizontal lines represent the zero-shear rate predictions in the excluded volume limit, reproduced from ref. 24.

this result, and the values for a_η and a_ψ from Table I into Eq. (26), and using standard methods for the estimation of error propagation, leads to $U_{\Psi\eta} = 0.568 \pm 0.038$. Thus, the universal ratio $U_{\Psi\eta}$ decreases from a zero shear rate value of 0.771 ± 0.009, to a shear rate independent value of 0.568 ± 0.038 in the limit of large shear rates.

Figure 6 displays the dependence of $U_{\Psi\eta}$ on β, obtained by carrying out Brownian dynamics simulations (open circles), and with the Gaussian approximation (squares). In each case, the symbols denote values that have been calculated using Eq. (24), with the excluded volume limit values substituted for all the quantities on the right hand side. The dashed curves have been obtained from Eq. (25), using mean values for the Carreau-Yasuda model parameters given in Table I. Unlike in the case of *exact* Brownian dynamics simulations, since $m_\psi \neq 2m_\eta$ in the Gaussian approximation, $U_{\Psi\eta}$ does not reach a constant value in the limit of large β.

Perhaps the most celebrated result of the study of excluded volume interactions in dilute polymer solutions is the observation that at large molecular weights, the equilibrium root-mean-square radius of gyration of the polymer coil, R_{g}, scales with molecular weight as a power law, $R_{\mathrm{g}} \sim M^\nu$, where ν is a universal exponent, independent of the particular polymer-solvent system. Pierleoni and Ryckaert[15] have shown recently, by calculating the structure factor for bead-spring chains with up to 300 beads, that in the presence of excluded volume interactions, two distinct regimes can be identified in the structure of a linear polymer chain undergoing shear flow. At large length scales, the polymer coil has a Rouse-like behavior, while at small length scales, where the flow field has not yet

distorted the isotropic coil structure, the polymer coil exhibits typical self-avoiding statistics. In the light of these observations we expect, therefore, that in the limit of infinite chain length, the scaling exponent ν will remain unaltered from its equilibrium value, since, at any particular shear rate, more and more polymer length scales will be smaller than the smallest length scale probed by the flow field. Recently, Kumar and Prakash[24] have obtained the value of ν at equilibrium, by exploiting a unique feature of the solution to the excluded volume problem. We show here that the same procedure can also be applied to find the value of ν in the presence of shear flow. In order to do so, however, it is necessary to make a few introductory remarks.

While the power law scaling of R_g with chain length N occurs only in the excluded volume limit, it is common to describe the dependence of R_g on N, at all values of chain length, with an apparent power law, $R_g \sim N^{\nu_{\text{eff}}}$, with ν_{eff} representing an effective exponent that approaches its critical value ν, as $N \to \infty$. Schafer and coworkers[8,34] have shown that the manner in which ν_{eff} approaches its asymptotic limit is strongly dependent on the magnitude of the parameter z^* relative to its *fixed point* value z_f^*. Discussions of the origin of the fixed point, and its significance can be found in treatises on renormalization group methods.[6,7,8] Basically, the existence of power law behavior in the excluded volume limit, such as the one observed for R_g, is intimately connected to the existence of a fixed point value for the parameter z^*. Schafer and coworkers have shown, using both renormalization group methods, and Monte Carlo simulations, that $\nu_{\text{eff}} \to \nu$ on two distinct branches, (i) the strong-coupling branch corresponding to $z^* > z_f^*$, and (ii) the weak-coupling branch corresponding to $z^* < z_f^*$. On the weak-coupling branch, for increasing values of N (or equivalently z), ν_{eff} approaches ν from below, increasing rapidly at first before approaching the asymptotic value very gradually. On the other hand, on the strong-coupling branch, ν_{eff} approaches ν from above, decreasing rapidly before approaching the asymptotic value slowly. Kumar and Prakash[24] have shown that Brownian dynamics simulations are able to capture the existence of the dual branched structure of the solution to the excluded volume problem. Furthermore, they show that this distinctive feature of the solution implies that at fixed values of z and d^*, a plot of ν_{eff} versus z^*, for a range of values spanning the fixed point, has a characteristic shape exhibiting a marked inflection point, from which one can obtain both the fixed point z_f^*, and the critical exponent ν (see Fig. 11 in ref. 24). In particular, they found that at equilibrium, $\nu = 0.6$, and $0.28 \leq z_f^* \leq 0.3$.

By collecting data on R_g as a function of N, at various constant values of the parameters z^*, and β, the value of ν_{eff}, at particular values of z and d^*, can be calculated with the help of the expression, $\nu_{\text{eff}} = \partial \ln R_g / \partial \ln N$. The symbols in Fig. 7 have been obtained in this manner, for two representative values of the characteristic shear rate β. It is clear from the figure that the dual branched
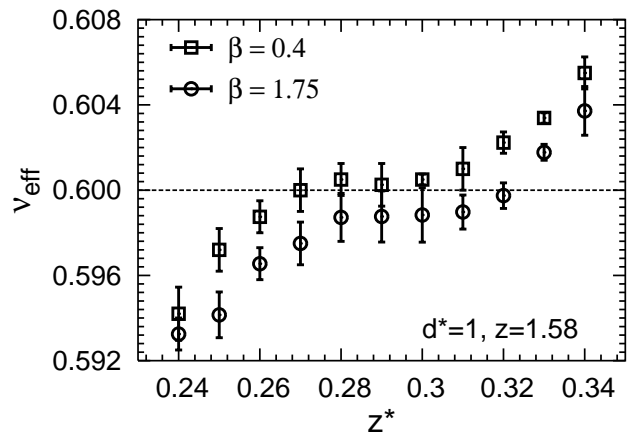

FIG. 7: The effective exponent ν_{eff} as a function of the strength of excluded volume interactions z^*, predicted by Brownian dynamics simulations, at two different vales of the shear rate β.

structure of the solution persists into the non-equilibrium regime, and the characteristic shape of the dependence of ν_{eff} on z^*, observed at equilibrium, is preserved at finite values of the shear rate. The point of inflection, for the data corresponding to $\beta = 0.4$, clearly indicates that both z_f^* and ν are unaltered from their equilibrium values. At $\beta = 1.75$, while z_f^* lies in the same interval as at equilibrium, there is a small decrease in the value of ν, arising perhaps due the relatively small values of N used to acquire the data. The results displayed in Fig. 7 are consistent with the argument that, for chains having sufficiently large number of beads, regardless of the characteristic shear rate β, there exists a local length scale below which the beads do not experience flow, and are effectively at equilibrium.

It is appropriate now to discuss the earlier observation in Fig. 3 that the *exact* crossover functions for $\eta_p/\eta_{p,0}$ and $\Psi_1/\Psi_{1,0}$, in the limit of large z, do not approach the asymptotic predictions obtained in the excluded volume limit. Kumar and Prakash[24] have speculated, in connection with a similar observation made earlier for universal equilibrium and linear viscoelastic ratios, that the origin of this behavior might lie in the fundamental difference between systems described by the crossover region, and those that correspond to the excluded volume limit. As pointed out earlier, since the crossover behavior has been obtained by keeping z constant as $N \to \infty$ (which implies that $z^* \to 0$, and $T \to T_\theta$), points on a crossover curve correspond to systems, (i) that are infinitesimally close to the θ-temperature, and (ii) that satisfy the criteria for belonging to the weak-coupling branch. On the other hand, since the excluded volume limit behavior has been obtained for systems with a finite value of z^*, they correspond to systems, (i) with a non-zero difference between T and T_θ, and (ii) that belong to either the weak or the strong-coupling branch. Interestingly, it was shown in ref. 24 that, at equilibrium, the Gaussian approximation

does not possess the dual-branched structure of the exact solution. We have not examined here whether such is the case even at finite shear rates. Nevertheless, as pointed out previously, both at equilibrium and at steady state, the large z crossover behavior of the Gaussian approximation coincides with the behavior in the excluded volume limit, unlike in the case of the exact solution.

A number of studies aimed at predicting the orientation angle and orientation resistance in shear flow, associated with various tensorial quantities, as a function of the shear rate, have been carried out previously.[15,22,32,35,36] The general consensus is that these quantities are universal properties of a dilute polymer solution, in the sense that, at the same reduced shear rate β, chains of different lengths have the same orientation angles and resistances. The universal dependence of χ_G and m_G on β, predicted by the present Brownian dynamics simulations in the excluded volume limit, will be presented shortly below. However, the universal shear rate dependence of the orientation angle χ_τ, and the orientation resistance m_τ (with the expected power law behavior at large values of β), can be derived in a straightforward manner from the results that have been obtained above for the shear rate dependence of the viscometric functions in the excluded volume limit, namely, Eqs. (23).

Substituting the expressions for the viscometric functions, Eqs. (9), into the defining expressions for χ_τ and m_τ, Eq. (15), and using the Carreau-Yasuda model, and the relation between $\dot{\gamma}$ and β, leads to the following expressions,

$$\cot(2\chi_\tau) = \frac{U_{\Psi\eta,0}}{2} \frac{(\Psi_1/\Psi_{1,0})}{(\eta_p/\eta_{p,0})} \beta \qquad (27)$$

$$= \frac{U_{\Psi\eta,0}}{2} \frac{[1 + (a_\psi\beta)^{n_\psi}]^{(m_\psi/n_\psi)}}{[1 + (a_\eta\beta)^{n_\eta}]^{(m_\eta/n_\eta)}} \beta \qquad (28)$$

$$m_\tau = \frac{2}{U_{\Psi\eta,0}} \frac{(\eta_p/\eta_{p,0})}{(\Psi_1/\Psi_{1,0})} \qquad (29)$$

$$= \frac{2}{U_{\Psi\eta,0}} \frac{[1 + (a_\eta\beta)^{n_\eta}]^{(m_\eta/n_\eta)}}{[1 + (a_\psi\beta)^{n_\psi}]^{(m_\psi/n_\psi)}} \qquad (30)$$

On using the relation $m_\psi = 2m_\eta$, Eqs. (28) and (30) simplify to the following power law dependencies of $\cot(2\chi_\tau)$ and m_τ on β, in the limit of large β,

$$\cot(2\chi_\tau) = \frac{U_{\Psi\eta,0}}{2} \left(\frac{a_\psi^2}{a_\eta}\right)^{m_\eta} \beta^{1+m_\eta} \qquad (31)$$

$$m_\tau = \frac{2}{U_{\Psi\eta,0}} \left(\frac{a_\eta}{a_\psi^2}\right)^{m_\eta} \beta^{-m_\eta} \qquad (32)$$

Since both renormalization group theory,[9,23] and the current Brownian dynamics simulations suggest $m_\eta \approx -0.25$ (see Table I), Eqs. (31) and (32) indicate that $\cot(2\chi_\tau)$ grows approximately as $\beta^{0.75}$, while m_τ has a weaker dependence, growing approximately as $\beta^{0.25}$, in the limit of large β. These predictions are of course restricted to the
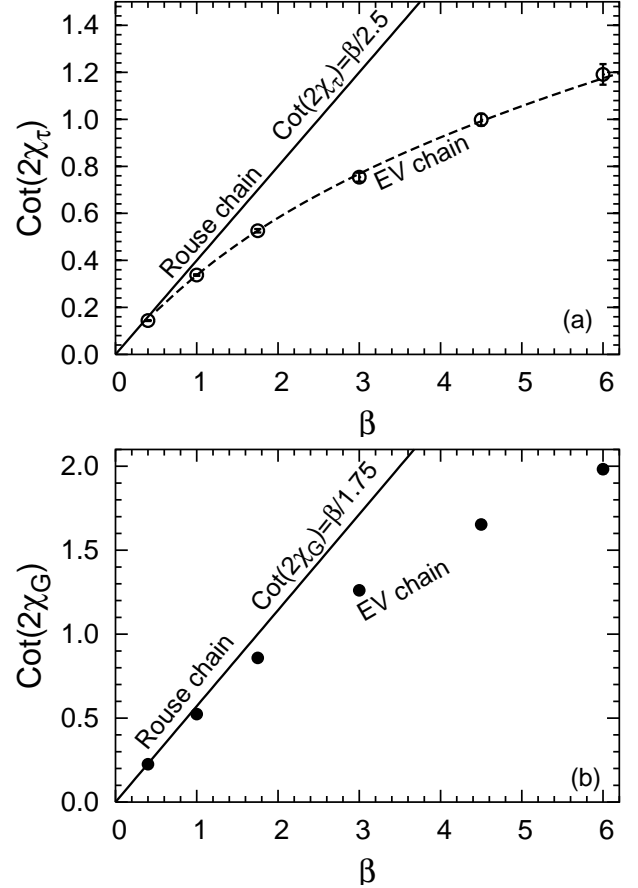

FIG. 8: Universal dependence of the cotangent of the orientation angles, (a) χ_τ (open circles), and (b) χ_G (filled circles), on the characteristic shear rate β, in the excluded volume limit, obtained by Brownian dynamics simulations. The dashed curve through the χ_τ data has been drawn using Eq. (28), with parameter values reported in Table I. The solid lines are the predictions of the Rouse model.

influence of excluded volume interactions on these quantities, and a thorough comparison with experiment requires the incorporation of hydrodynamic interaction effects. Bossart and Öttinger[32] and Cifre and de la Torre[22] have shown previously that the presence of hydrodynamic interactions also leads to shear rate dependent orientation angles and resistances. Interestingly, however, in contrast to the prediction obtained here in the presence of excluded volume interactions alone, they find that at large values of β, the orientation resistance m_τ *decreases* with increasing shear rate. As is well known, the presence of hydrodynamic interactions leads to the prediction of *shear thickening* at large values of β.[37] It is clear from Eq. (32), that a positive value of the exponent m_η, would explain the observation of Bossart and Öttinger, and Cifre and de la Torre.

Figures 8 display the shear rate dependence of the orientation angles obtained here by Brownian dynamics simulations in the excluded volume limit. In the case
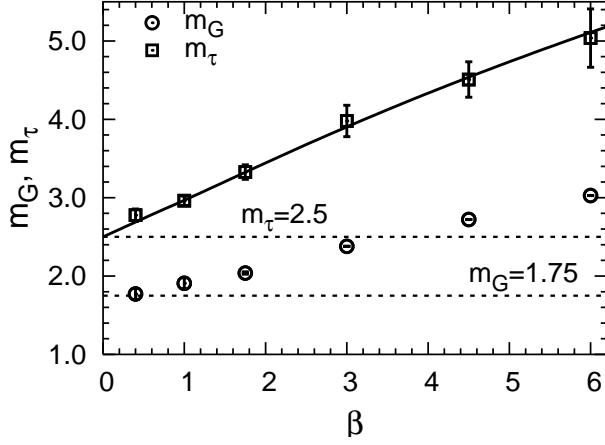
FIG. 9: Universal dependence of the orientation resistances m_τ (squares) and m_G (circles), on the characteristic shear rate β, in the excluded volume limit. The line through the m_τ data has been drawn using Eq. (30), with parameter values reported in Table I. The horizontal lines are the predictions of the Rouse model.

of $\cot(2\chi_\tau)$, values for $\eta_p/\eta_{p,0}$ and $\Psi_1/\Psi_{1,0}$, obtained at various values of β, in the excluded volume limit, have been substituted on the right hand side of Eqs. (27), with $U_{\Psi\eta,0} = 0.771 \pm 0.009$. On the other hand, $\cot(2\chi_G)$ has been evaluated by accumulating finite chain data using Eq. (16), at a constant value of $z^* = 0.28$ (the fixed point value), followed by extrapolation to the long chain limit. Comparison with the Rouse model (which predicts a linear dependence on β in each case), clearly indicates that the presence of excluded volume interactions leads to a weakening of the alignment of the polymer coil in the flow direction. This has been observed previously both theoretically,[15] and experimentally.[38] Since, at the same shear rate β, $\cot(2\chi_G) > \cot(2\chi_\tau)$, the tensor $\boldsymbol{G}$ is more easily oriented than $\boldsymbol{\tau}^{\text{p}}$.

Figure 9 displays the universal dependence of the orientation resistances m_G and m_τ, in the excluded volume limit, on β. As in the case of χ_τ, the orientation resistance m_τ has been obtained by substituting known values on the right hand side of Eq. (29). On the other hand, m_G has been obtained from the Brownian dynamics simulation data for $\cot(2\chi_G)$, displayed in Fig. 8(b), by using the defining expression, $m_G = \beta/\cot(2\chi_G)$. It is evident from the figure that both m_G and m_τ increase with β, indicating that it gets increasingly difficult to orient the polymer coil with increasing shear rate. This has been previously predicted,[39] and observed experimentally at relatively low values of β.[40] The fact that $\boldsymbol{G}$ is more easily oriented than $\boldsymbol{\tau}^{\text{p}}$ can also be seen from the behavior of the orientation resistances m_G and m_τ, since $m_\tau > m_G$, for all values of β. As pointed out previously by Bossart and Öttinger,[32] flow birefringence experiments (which measure χ_τ), reflect orientational ordering on length scales smaller than those probed by light scattering experiments (which measure χ_G). Since smaller length scales are less

affected by flow, they exhibit greater resistance to orientational ordering, leading to the observed relative magnitudes of m_G and m_τ.

It is of particular interest to examine the universal values of the orientation resistances in the limit of zero shear rate, namely, $m_{G,0}$ and $m_{\tau,0}$, since a number of studies have been confined to the low shear rate regime. Bossart and Öttinger,[32] and Pierleoni and Ryckaert[39] have argued previously that the effect of excluded volume interactions on the orientation resistance is negligible. Bossart and Öttinger,[41] have found, from careful experiments, that in a good solvent (polystyrene in bromobenzene), $m_{\tau,0} = 3.74 \pm 0.28$, compared to the value of 3.13 ± 0.42 in a theta solvent (polystyrene in 4-bromo-α-benzyl alcohol). Given the magnitude of the error bars, it can only be concluded that $m_{\tau,0}$ is probably *larger* in a good solvent than in a theta solvent. It must be borne in mind that both these values reflect the influence of hydrodynamic interactions. In the present instance, where only the influence of excluded volume interactions is considered, the value of $m_{\tau,0}$ can be obtained from the following expression,

$$m_{\tau,0} = \frac{2}{U_{\Psi\eta,0}} \qquad (33)$$

which is derivable from Eq. (29) in the limit of zero shear rate. Using the previously established *exact* Brownian dynamics simulations value of $U_{\Psi\eta,0} = 0.771 \pm 0.009$,[24] leads to, $m_{\tau,0} = 2.594 \pm 0.030$, which is marginally larger than the Rouse value of 2.5. Using non-equilibrium molecular dynamics simulations of bead-spring chains with FENE springs, Aust et al.[36] have estimated $m_{\tau,0} = 2.4 \pm 0.3$. Interestingly, in spite of the fact that the solvent is treated explicitly in these simulations, and consequently hydrodynamic interactions are taken into account, the predicted value is not significantly different from the pure excluded volume prediction obtained here. It is worth noting that Bossart and Öttinger,[32] who used the Gaussian approximation, and de la Torre and co-workers,[22,35] who used Brownian dynamics simulations with hydrodynamic interactions, report the values: $m_{\tau,0} \approx 3.57$, and $m_{\tau,0} \approx 3.5$, respectively—both of which are substantially different from the prediction of the Rouse model. While an improvement in solvent quality seems to increase $m_{\tau,0}$ fractionally, our results seem to suggest that it *decreases* $m_{G,0}$ fractionally. By fitting the m_G data in Fig. 9 with a least squares third order polynomial, and extrapolating to $\beta \to 0$, we find that in the excluded volume limit, $m_{G,0} = 1.69 \pm 0.03$, which is slightly smaller than the Rouse prediction of $m_{G,0} = 1.75$. The value obtained here is in good agreement with the explicit solvent non-equilibrium molecular dynamics simulations of Aust et al.[36] and the results of renormalization group calculations,[32] both of which predict $m_{G,0} = 1.7$. Since these studies account for hydrodynamic interactions, it is clear that hydrodynamic interactions have no effect on $m_{G,0}$. Pierleoni and Ryckaert have also observed a similar pattern when comparing

their explicit solvent molecular dynamics simulations[39] with their Brownian dynamics simulations (in which only excluded volume interactions were taken into account).[15] It is well known that hydrodynamic interactions have a significant influence on *dynamic* properties, but have no influence on *static* properties, since the equilibrium distribution function is unaltered in their presence. This suggests, perhaps not surprisingly, that $m_{G,0}$ is static property, while $m_{\tau,0}$ is a dynamic property.

IV. CONCLUSIONS

Results of a detailed Brownian dynamics simulations study, of a polymer solution undergoing steady shear flow, have been presented. The polymer molecule has been modelled by a bead-spring chain, and a narrow Gaussian excluded volume potential, that acts between pairs of beads, has been used to mimic the influence of solvent quality.

Material properties have been shown to become independent of the range of excluded volume interactions d^*, and the number of beads N, in the limit of large N. Furthermore, it has been found that master plots are obtained when, (i) the influence of the strength of excluded volume interactions is interpreted in terms of the solvent quality parameter $z = z^* \sqrt{N}$, and (ii) the dependence on the shear rate $\dot{\gamma}$ is interpreted in terms of the characteristic non-dimensional shear rate, β. In this work, we have explored the universal dependence of the non-dimensional viscosity ratio $(\eta_{\mathrm{p}}/\eta_{\mathrm{p},0})$, the non-dimensional first normal stress difference ratio $(\Psi_1/\Psi_{1,0})$, the orientation angles χ_τ and χ_G, and the orientation resistances m_τ and m_G, on the characteristic shear rate β and the solvent quality z.

The extent of shear thinning has been found to increase as z increases (Figs. 2). However, the incremental increase in shear thinning saturates as z increases (Figs. 3). The existence of universal viscometric ratio versus shear rate curves, independent of all model parameters, in the excluded volume limit, $z \to \infty$, has been verified (Figs. 5). The shear rate dependence of both the universal viscometric ratios has been found to be well described by the Carreau-Yasuda model, with power law decay exponents at large values of β, that are in close agreement with values predicted by renormalization group theory (Table. I).

The asymptotic values of the exact crossover functions for $(\eta_{\mathrm{p}}/\eta_{\mathrm{p},0})$ and $(\Psi_1/\Psi_{1,0})$, in the limit of large z, are found not to approach the universal predictions obtained in the excluded volume limit, unlike previous predictions of the Gaussian approximation (Figs. 3).

The shear rate dependence of the universal ratio $U_{\Psi\eta}$ has been obtained in the excluded volume limit. The ratio is found to decrease from the zero shear rate value of 0.771 ± 0.009, to a constant value of 0.568 ± 0.038, in the limit of large shear rates (Fig. 6).

The dual branched structure of the solution, elucidated recently by Scäfer and co-workers,[8,34] and shown to be captured by Brownian dynamics simulations at equilibrium,[24] has been found to persist into the non-equilibrium regime. As in the equilibrium case, this distinctive structure has been exploited here to obtain an estimate of both the fixed point of the strength of excluded volume interactions, and the critical exponent ν. Both quantities are found to remain unaltered in the presence of shear flow (Fig. 7).

The universal dependence of χ_τ, χ_G, m_τ and m_G, on β, in the excluded volume limit, has been obtained. The presence of excluded volume interactions has been shown to weaken the alignment of polymer coils in the flow direction (Figs. 8). Of the two tensors, the radius of gyration tensor $\boldsymbol{G}$ is found to be more easily oriented than $\boldsymbol{\tau}^{\mathrm{P}}$ (Fig. 9). The power law shear rate dependence of χ_τ $(\sim \beta^{0.75})$ and m_τ $(\sim \beta^{0.25})$, in the limit of large shear rate, has been obtained by exploiting the Carreau-Yasuda model fit of the universal viscometric functions. The presence of excluded volume interactions leads to a marginal increase in $m_{\tau,0}$, while marginally reducing $m_{G,0}$.

[*] Present address: Department of Physics, POSTECH San 31, Hyoja-dong, Nam-gu, Pohang, Kyungbuk, 790-784 Republic of Korea

[†] Electronic address: ravi.jagadeeshan@eng.monash.edu.au

[1] Y. Miyaki and H. Fujita, Macromolecules **14**, 742 (1981).

[2] P. Vidakovic and F. Rondelez, Macromolecules **18**, 700 (1985).

[3] R. C. Hayward and W. W. Graessley, Macromolecules **32**, 3502 (1999).

[4] M. Bercea, C. Ioan, S. Ioan, B. C. Simionescu, and C. I. Simionescu, Progress in Polymer Science **24**, 379 (1999).

[5] M. Doi and S. F. Edwards, *The Theory of Polymer Dynamics* (Oxford University Press, New York, 1986).

[6] K. F. Freed, *Renormalization Group Theory of Macromolecules* (Wiley, New York, 1987).

[7] J. des Cloizeaux and G. Jannink, *Polymers in Solution, Their Modeling and Structure* (Oxford Science Publishers, 1990).

[8] L. Schäfer, *Excluded Volume Effects in Polymer Solutions* (Springer-Verlag, Berlin, 1999).

[9] H. C. Öttinger, Phys. Rev. A **40**, 2664 (1989).

[10] W. Zylka and H. C. Öttinger, Macromolecules **24**, 484 (1991).

[11] N. C. Andrews, A. K. Doufas, and A. J. McHugh, Macromolecules **31**, 3104 (1998).

[12] J. G. H. Cifre and J. G. de la Torre, J. Rheol. **43**, 339 (1999).

[13] J. R. Prakash and H. C. Öttinger, Macromolecules **32**, 2028 (1999).

[14] L. Li and R. G. Larson, Rheol. Acta **39**, 419 (2000).

[15] C. Pierleoni and J.-P. Ryckaert, J. Chem. Phys. **113**, 5545 (2000).

[16] R. M. Jendrejack, M. D. Graham, and J. J. de Pablo, J. Chem. Phys. **116**, 7752 (2002).

[17] J. R. Prakash, Chem. Eng. Sci. **56**, 5555 (2001).

[18] J. R. Prakash, Macromolecules **34**, 3396 (2001).

[19] J. R. Prakash, J. Rheol. **46**, 1353 (2002).

[20] R. Prabhakar and J. R. Prakash, J. Rheol. **46**, 1191 (2002).

[21] R. Prabhakar and J. R. Prakash, J. Non-Newtonian Fluid Mech. **116**, 163 (2004).

[22] J. G. H. Cifre and J. G. de la Torre, Macromol. Theory Simul. **13**, 273 (2004).

[23] H. C. Öttinger, Phys. Rev. A **41**, 4413 (1990).

[24] K. S. Kumar and J. R. Prakash, Macromolecules **36**, 7842 (2003).

[25] J. J. L. Cascales and J. G. de la Torre, Polymer **32**, 3359 (1991).

[26] K. D. Knudsen, J. G. de la Torre, and A. Elgsaeter, Polymer **37**, 1317 (1996).

[27] R. M. Jendrejack, M. D. Graham, and J. J. de Pablo, J. Chem. Phys. **113**, 2894 (2000).

[28] M. Kröger, A. Alba-Pérez, M. Laso, and H. C. Öttinger, J. Chem. Phys. **113**, 4767 (2000).

[29] H. C. Öttinger, *Stochastic Processes in Polymeric Fluids* (Springer-Verlag, 1996).

[30] R. B. Bird, C. F. Curtiss, R. C. Armstrong, and O. Hassager, *Dynamics of Polymeric Liquids - Volume 2: Kinetic Theory* (John Wiley, New York, 1987), 2nd ed.

[31] R. B. Bird, R. C. Armstrong, and O. Hassager, *Dynamics of Polymeric Liquids - Volume 1: Fluid Mechanics* (John Wiley, New York, 1987), 2nd ed.

[32] J. Bossart and H. C. Öttinger, Macromolecules **28**, 5852 (1995).

[33] A. Iniesta and J. G. de la Torre, J. Chem. Phys. **92**, 2015 (1990).

[34] P. Grassberger, P. Sutter, and L. Schäfer, J. Phys. A: Math. Gen. **30**, 7039 (1997).

[35] K. D. Knudsen, A. Elgsaeter, J. J. L. Cascales, and J. G. de la Torre, Macromolecules **26**, 3851 (1993).

[36] C. Aust, M. Kröger, and S. Hess, Macromolecules **32**, 5660 (1999).

[37] J. R. Prakash, in *Advances in flow and rheology of non-Newtonian fluids*, edited by D. A. Siginer, D. D. Kee, and R. P. Chhabra (Elsevier Science, Rheology Series, Amsterdam, 1999), pp. 467–517.

[38] E. C. Lee and S. J. Muller, Polymer **40**, 2501 (1999).

[39] C. Pierleoni and J.-P. Ryckaert, Macromolecules **28**, 5097 (1995).

[40] A. Link and J. Springer, Macromeolecules **26**, 464 (1993).

[41] J. Bossart and H. C. Öttinger, Macromolecules **30**, 5527 (1997).

[42] Italics are used here throughout to qualify the term "exact", with a view to indicating the fact that results are exact only to within the numerical error bars of the simulations. These errors can, of course, be made arbitrarily small by suitably increasing the number of simulation trajectories.